

Let's push things forward: disruptive technologies and the mechanics of tissue assembly

Cite this: *Integr. Biol.*, 2013, 5, 1162

Victor D. Varner^a and Celeste M. Nelson^{*ab}

Although many of the molecular mechanisms that regulate tissue assembly in the embryo have been delineated, the physical forces that couple these mechanisms to actual changes in tissue form remain unclear. Qualitative studies suggest that mechanical loads play a regulatory role in development, but clear quantitative evidence has been lacking. This is partly owing to the complex nature of these problems – embryonic tissues typically undergo large deformations and exhibit evolving, highly viscoelastic material properties. Still, despite these challenges, new disruptive technologies are enabling study of the mechanics of tissue assembly in unprecedented detail. Here, we present novel experimental techniques that enable the study of each component of these physical problems: kinematics, forces, and constitutive properties. Specifically, we detail advances in light sheet microscopy, optical coherence tomography, traction force microscopy, fluorescence force spectroscopy, microrheology and micropatterning. Taken together, these technologies are helping elucidate a more quantitative understanding of the mechanics of tissue assembly.

Received 26th April 2013,
Accepted 13th July 2013

DOI: 10.1039/c3ib40080h

www.rsc.org/ibiology

Insight, innovation, integration

Understanding how tissues are assembled in the embryo is of vital importance to the fields of tissue engineering and medicine. Fundamentally, this process – termed morphogenesis – is a physical one: tissues are molded through the action of mechanical forces, which makes investigations of this process inherently interdisciplinary. Ideas from the physical sciences are yielding novel, quantitative *insight* into the process of morphogenesis – both in the embryo and in culture. Here, we discuss *innovative*, disruptive technologies that are enabling a more detailed study of the mechanics of tissue assembly. These techniques *integrate* the tools of biomedical imaging and microfabrication with concepts from both continuum and statistical mechanics.

Introduction

For centuries scientists have sought to determine how complex biological structures are sculpted from the raw material of a single cell, a process termed morphogenesis.¹ Understanding how tissues are assembled in the developing embryo yields insight for translational fields as varied as tissue engineering and pediatric medicine. Tissue engineers seek to design and construct artificial tissues in culture and thereby recapitulate morphogenesis in the laboratory.² Clinicians, meanwhile, work to prevent and treat congenital disorders, conditions that often arise in neonates as defects of form: morphogenesis gone horribly and catastrophically awry. A neural tube fails to close and causes spina bifida;¹ an esophagus errantly connects into the windpipe and produces esophageal atresia.³

Since the revolutionary discovery of the structure of DNA by Watson and Crick in 1953,⁴ scientists have primarily worked to characterize the biochemical signals that underlie tissue assembly in the embryo.¹ This important work has helped elucidate the vast signaling and gene regulatory networks that pattern the early embryo and drive the differentiation of organ-specific cell types.^{5,6} Morphogenesis, however, necessarily involves mechanical forces,⁷ and the physical mechanisms which link molecular signals to actual deformations in the embryo remain largely unclear. Moreover, it is evident that mechanical forces not only mold embryonic tissues, they also play a crucial regulatory role during development.^{8–10} Cells actively modify and respond to their physical microenvironment. Yet how forces are coordinated within an intact tissue, how cells sense and respond to physical cues, and how mechanical loads regulate cell behavior and gene expression remain open questions.¹¹ These problems are unavoidably complex, but significant early progress has been made by quantifying some of the mechanical forces that drive tissue morphogenesis, both in the embryo^{12–15} and in culture.^{16,17}

^a Department of Chemical & Biological Engineering, Princeton University, Princeton, NJ 08544, USA

^b Department of Molecular Biology, Princeton University, 303 Hoyt Laboratory, William Street, Princeton, NJ 08544, USA. E-mail: celesten@princeton.edu; Fax: +1 609-258-1247; Tel: +1 609-258-8851

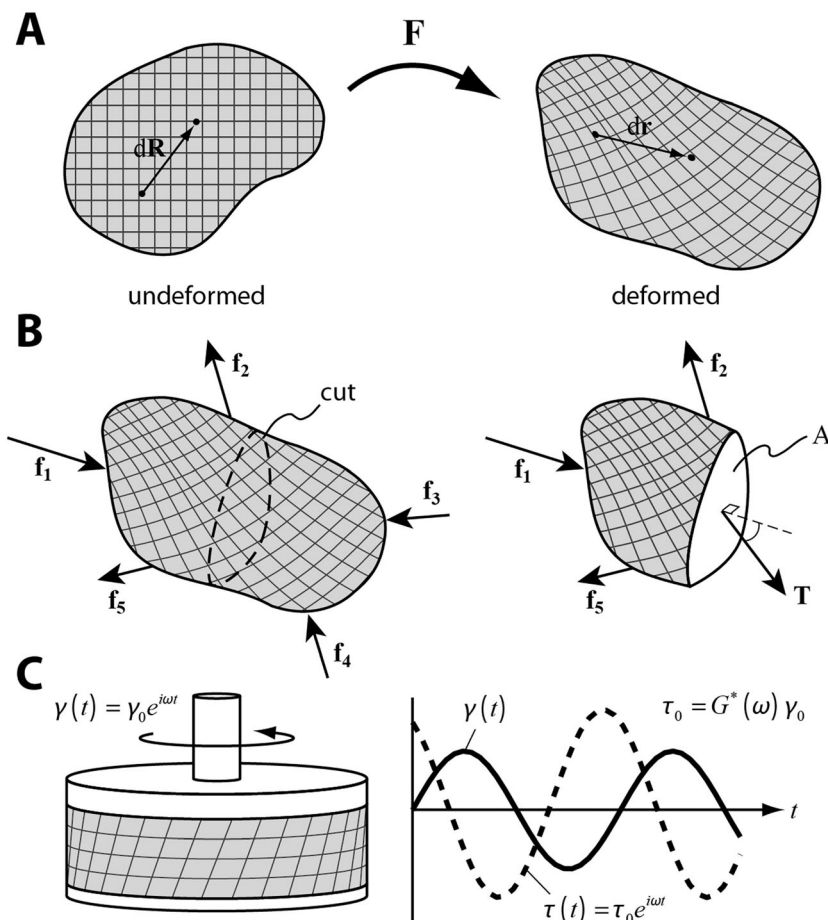


Fig. 1 Schematic depicting the three parts of any continuum mechanics problem: (A) kinematics, (B) equilibrium, and (C) constitutive properties. (A) Kinematics describes the motion of a material body. This can be expressed mathematically using the deformation gradient tensor F , which transforms the differential position vector $d\mathbf{R}$ in the undeformed configuration into the deformed differential position vector $d\mathbf{r}$ by $d\mathbf{r} = F \cdot d\mathbf{R}$. (B) Morphogenetic processes can be treated quasi-statically. In the absence of body forces, equilibrium relations dictate that the sum of all traction forces (internal and external) acting on a body be equal to zero (*i.e.*, $\Sigma \mathbf{f}_1 + \mathbf{f}_2 + \mathbf{f}_3 + \mathbf{f}_4 + \mathbf{f}_5 = 0$ and $\Sigma \mathbf{f}_1 + \mathbf{f}_2 + \mathbf{f}_5 + \mathbf{T} = 0$). Traction stress is defined by the traction force \mathbf{T} acting over the reference area A . In general, there are a variety of different mathematical descriptions for the stress-state,²⁰ which depend on the selected reference configuration. It is important to note that *forces* – not stresses – balance in equilibrium. (C) Forces and deformations are linked by the constitutive properties of a material. Mechanical tests using a parallel plate rheometer relate to an oscillatory shear stress $\gamma(t)$ to an oscillatory stress $\tau(t)$, which are coupled by the complex viscoelastic shear modulus $G^*(\omega)$.

Continuum mechanical approaches[†] have given insight into the physical behavior of biological systems across length scales ranging from the level of cytoskeletal proteins to the level of the tissue.¹⁸ Importantly, each continuum mechanics problem consists of three sets of governing equations:^{19,20}

- Kinematics: the deformations experienced by a material (Fig. 1A);
- Equilibrium relations: the balance[‡] of mechanical forces acting upon (and within) a material (Fig. 1B);

[†] In a continuum mechanical framework, any discrete material structures are lumped into continuous field properties, and the material is treated as a continuum of particles. It is thus assumed that the deformations of interest occur at length scales sufficiently greater than that of any discrete material structure.

[‡] During morphogenesis inertial effects are negligible. The problem is treated as quasi-static, and the sum of all forces is taken equal to zero. Importantly, equilibrium relations are satisfied both locally (*i.e.* at any given material point) and globally in the material.

- Constitutive properties: the experimentally determined relations that couple deformations to applied loads for a material under specific conditions (Fig. 1C).

Here, we consider novel disruptive technologies that have revolutionized each of these areas, and thus our ability to characterize the mechanics of tissue assembly. Specifically, we describe (i) new imaging technologies that allow quantification of the kinematics of morphogenesis, (ii) microscopy techniques which enable the dynamic measurement of forces in intact cells and tissues, and (iii) microrheological methods that permit non-invasive characterization of the viscoelastic behavior of biological materials. Lastly, we consider how each of these techniques might be employed to study tissue assembly in the context of three-dimensional (3D) micropatterned tissues – yet another disruptive technology which offers unprecedented control of the tissue microenvironment.

Imaging the kinematics of tissue assembly

Developing organs and tissues arise from simple primordia such as tubes or sheets. These elementary structures are then elaborated into more complex forms as cells proliferate, rearrange and change shape. The ability to quantify the kinematics of these deformations is largely constrained by the extent to which they can be observed. Imaging morphogenesis within intact embryos, however, is extremely difficult.²¹ When observations are conducted over extended periods of time, fluorescent reporters can photobleach or cause phototoxicity. As embryos get larger (and thicker), it becomes progressively more challenging to resolve deeper tissues. In addition, intact mammalian embryos are notoriously difficult to culture *ex vivo*, especially at the later stages relevant for organogenesis, which leaves one with the daunting task of imaging morphogenesis in utero. Still, despite these obvious challenges, promising new imaging technologies including light sheet microscopy (LSM) and optical coherence tomography (OCT) are making 4D kinematic studies of tissue assembly possible.

First developed to study colloid chemistry,^{22,23} LSM illuminates a planar section of the imaging sample, which is then scanned through space to create a 3D reconstruction. This generates high-resolution images at high speed (175 million voxels per second for multiview LSM) and minimizes photo-damage to cells and tissues.²⁴ As a result, 3D reconstructions of entire embryos can be captured quickly (the imaging time for a *Drosophila* embryo is approximately 30 seconds^{24,25}), which makes LSM a promising tool for kinematic studies of tissue assembly. Quantifying morphogenetic deformations, however, involves tracking of fiducial tissue markers, such as adherent polystyrene microspheres or fluorescently labeled cells.²⁶ Since embryos typically undergo large changes in shape, sequential images must be captured with high temporal resolution to reliably track the motion of markers in time.

Imaging whole embryos using LSM was first demonstrated in fixed specimens,²⁷ but was later extended to living zebrafish embryos expressing fluorescent reporters^{28,29} (Fig. 2A). Since then, investigators have generated cell lineage maps for entire *Drosophila* embryos.^{24,25} If these lineage data are also used to quantify morphogenetic deformations during embryogenesis,^{15,30} it can be determined whether or not embryos undergo conserved tissue-level shape changes in the presence of significant cell lineage variability.

This kinematic description of embryogenesis also enables a more physical understanding of mutant phenotypes. The effects of specific mutations can be quantified by determining how mutant kinematics deviate from deformations observed in wild type embryos – differences that may not be discernable by morphology alone. In addition, considering entire embryos makes it possible to identify physical interactions between tissues that might be missed if a particular organ system or developmental event were considered in isolation. Lastly, global patterns of cell motion in the embryo could also be correlated with spatiotemporal changes in gene expression,^{31,32} which might identify new (non-intuitive) sources of progenitor cells during tissue assembly.

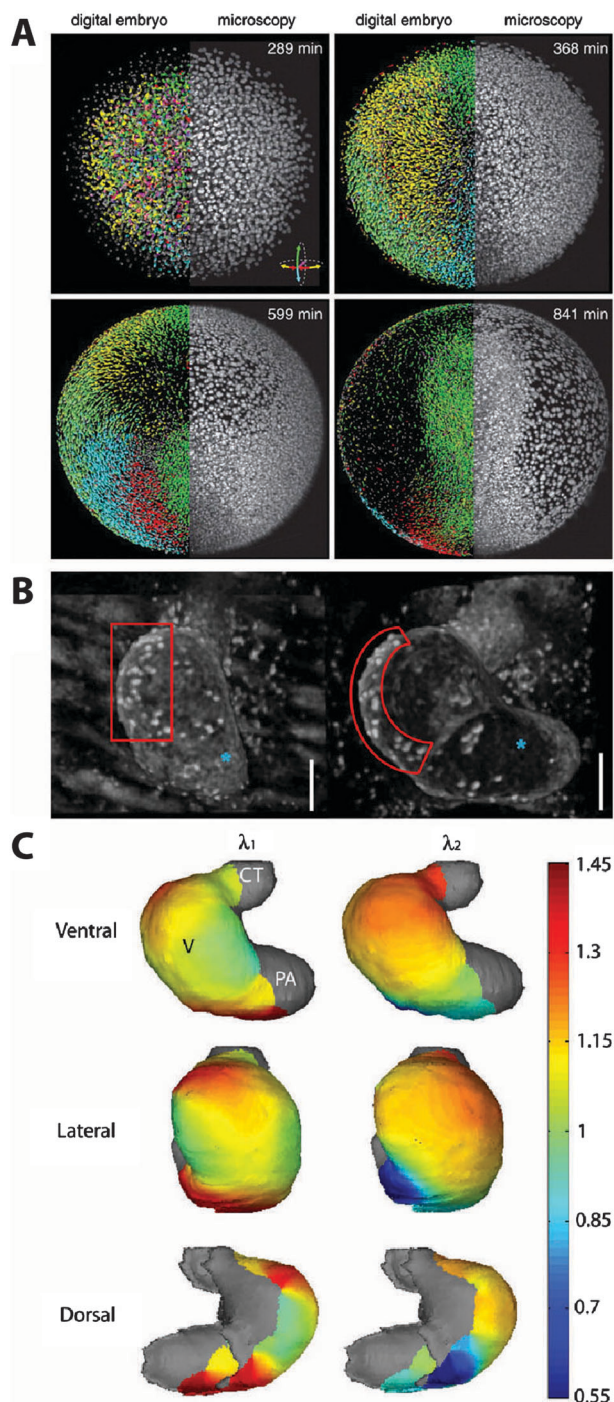


Fig. 2 Imaging the kinematics of tissue assembly. (A) Cell tracking data from a nuclear-labeled zebrafish embryo imaged over time using light sheet microscopy (LSM). Displacements of individual cells were reliably tracked in 4D. Adapted from Keller *et al.* (2008).²⁸ Reprinted with permission from AAAS. (B and C) Quantifying 3D surface deformations during cardiac looping in the early chicken embryo using optical coherence tomography (OCT). Circumferential (λ_1) and longitudinal (λ_2) stretch ratios were computed using tracked polystyrene microspheres adherent to the tissue. Adapted from Filas *et al.* (2007).³⁴ Reprinted with permission from ASME.

Alternatively, OCT has also been used in 4D studies of morphogenesis. Originally developed by Huang and colleagues,³³ OCT uses optical reflectance to generate 2D cross-sectional images

which can be assembled into 3D reconstructions. Conveniently, however, OCT does not require fluorescent reporters and is readily available from commercial vendors. Moreover, since fluorescence is not used, timelapse OCT experiments are not accompanied by some of the imaging complications associated with fluorescence microscopy (e.g. photobleaching, phototoxicity, etc.).

Several studies have used OCT to characterize the kinematics of tissue assembly. Polystyrene microspheres, adherent to the surface of embryonic tissue, can be tracked in time and used to quantify the deformations associated with cardiac looping in the early chicken embryo (Fig. 2B and C).³⁴ This technique, however, is limited to measuring surface deformations alone – and only in embryos that are readily accessible to manipulation. Moreover, surface beads can be sheared off when tissues come into contact and slide past one another, which can introduce artifacts in the analysis. Interestingly, however, OCT can also be used to also quantify the kinematics of fluid flow during development: for instance, both particle image velocimetry (PIV)³⁵ and the Doppler shift³⁶ have been used to study hemodynamics of the early embryonic heart.

Still, using either of these imaging modalities, computational image analysis is required to track the 4D displacements of multiple fiducial markers. Although commercial image processing software is available (e.g. Imaris, Volocity), custom image segmentation or tracking algorithms are often necessary. The details of such analyses are nuanced and complex, and spatial constraints preclude a detailed discussion of them here. The interested reader, however, is encouraged to consult excellent reviews on the subject by Megason and Fraser,²¹ Roeder and colleagues,³⁷ and Short and colleagues.³⁸

Regardless of the image analysis used, tissue deformations can be extracted from the motion of tracked markers using continuum field theory.^{20,39} For solid-like materials, a Lagrangian description of the deformation (or strain) field is typically used. In this case, the strain tensor E characterizes the deformation at each point in the tissue, and is computed with respect to a known reference configuration (Fig. 1A) by $E = \frac{1}{2}(\mathbf{F}^T \cdot \mathbf{F} - \mathbf{I})$, where the deformation gradient tensor F maps the undeformed differential position vector $d\mathbf{R}$ into the deformed vector $d\mathbf{r}$ by $d\mathbf{r} = \mathbf{F} \cdot d\mathbf{R}$, and \mathbf{I} represents the identity tensor. Alternatively, for fluid-like materials, an Eulerian description is employed and a tensorial description of the deformation rate is typically used.¶ Depending on the timescale of interest, biological tissues can exhibit solid-like or fluid-like behavior, so care must be taken when choosing an appropriate framework for quantifying the observed deformations.

Dynamically measuring forces in epithelial cells and tissues

During morphogenesis, tissues are assembled through the work of physical forces.⁴⁰ For mature tissues, these forces can

§ Unless microspheres are somehow injected ballistically into deeper tissues.

¶ A detailed description of these theoretical issues can be found in chapter 3 of Taber (2008).³⁰

be measured directly by macroscopic mechanical testing⁴¹ or estimated indirectly by measuring the deformations around punched circular holes.⁴² Both in the embryo and in the lab, however, tissue assembly occurs on much smaller length scales, and new tools are required to measure mechanical stress|| in these situations.⁴⁴ Recently, however, the advent of techniques such as traction force microscopy (TFM) and fluorescence force spectroscopy have made it possible to dynamically measure mechanical forces and stresses inside living cells and tissues.

TFM was first implemented by using the deformations of flexible substrata to estimate the traction stresses exerted by adherent cells in culture.⁴⁵ This approach was inherently interdisciplinary – cell culture meets elasticity. In these initial experiments, Harris and colleagues used the wrinkling of thin silicone films to estimate the traction stresses exerted by a variety of cell types, but could do so only qualitatively.⁴⁶ The mechanics of buckling films are complex and often involve large deformations,⁴⁷ which significantly complicates the problem of using the wrinkled geometry of the substratum to compute the traction forces.** Moreover, the spatial resolution of this initial technique was limited to the buckled wavelength of the thin film, and the wrinkles themselves were confined only to regional zones of compression.

Owing to these limitations, TFM was extended by embedding beads in the thin film and applying in-plane tensile stresses to prevent buckling.⁴⁸ Deformations could then be measured by tracking the motion of the embedded beads.^{49,50} If the mechanical properties of the substratum were known, a linear elastic framework could be used to construct a map of the cellular traction stresses.^{51–53} Importantly, since a unique set of discrete traction forces does not exist for a given (surface) deformation of the film, regularization techniques were required to compute the most likely distribution of forces.⁵² Substratum stiffness could be tuned by varying the amount of cross-linking within the synthetic gel,^{46,54} and investigators were able to quantify some of the mechanical forces involved in the locomotion of single migratory cells in culture (Fig. 3A).

Alternatively, single cells have also been cultured on arrays of flexible microfabricated posts of silicone rubber to compute the exerted traction forces.^{55–57} This assay has been used to precisely control the surface chemistry and contact area presented to adherent cells. In addition, computation of the resultant traction forces is made decidedly more straightforward.†† Still, the theoretical framework used in these calculations typically assumes that posts are slender and undergo small deflections,⁵⁹ which is often not the case for microposts made from silicone rubber.⁶⁰ In such cases, a more sophisticated analysis, which accounts for the effects of shear and/or large deformation, is required to more accurately estimate the

|| Strictly speaking, mechanical stresses cannot be measured directly, since stress is a purely mathematical construct – a tensorial quantity that represents a force acting over a particular reference area.^{19,20} For more on this, the interested reader should consult J. D. Humphrey's fantastic perspective piece on stresses and strains in cells and tissues.⁴³

** Although Harris and colleagues⁴⁶ did attempt to do so experimentally.

†† E.g. simple Eulerian beam theory is often used.⁵⁸

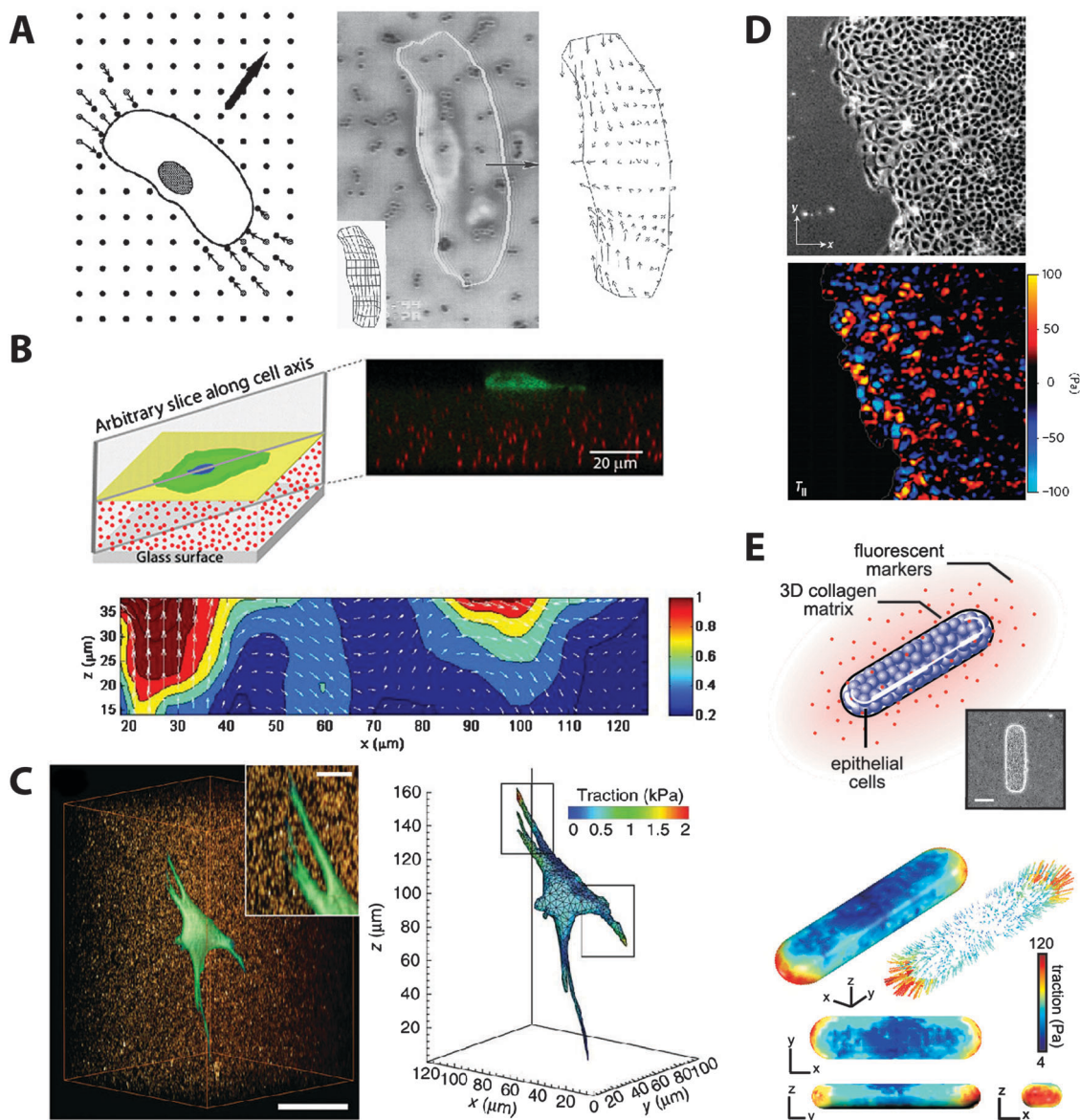


Fig. 3 Quantifying cellular forces using traction force microscopy (TFM). (A) Deformations of thin silicone membrane used to estimate traction forces exerted by individual cells in 2D culture. Adapted from Oliver *et al.* (1995).⁵⁰ Reprinted with permission. (B and C) extended to three dimensions by considering 3D hydrogel deformations during both (B) 2D and (C) 3D cell culture. Adapted from Maskarinec *et al.* (2009)⁶² and Legant *et al.* (2010).⁶⁹ Reprinted with permission. (D and E) Traction stresses measured during collective motion of both (D) 2D epithelial sheets and (E) 3D engineered epithelial tissues. Adapted from Trepats *et al.* (2009)⁶⁸ and Gjorevski and Nelson (2012).⁷⁰ Reprinted by permission from Macmillan Publishers Ltd and Elsevier, respectively.

traction forces.⁶⁰ In addition, the effect of substratum warping at the base of the micropost must often be considered.⁶¹

In each of these cases, analysis is restricted to individual cells in two dimensions. Recent work, however, has extended TFM to three dimensions by analyzing the 3D deformation field of the substratum during 2D cell culture^{62–65} (Fig. 3B). Although calculating the full 3D deformation field requires sophisticated tracking algorithms,⁶⁶ doing so abrogates the need for regularization, and computational approaches such as the finite element method can be used to calculate the resultant traction forces.⁶⁵

Others have also extended TFM to study the collective motion of groups of cells in 2D culture (Fig. 3C),^{67,68} and,

intriguingly, collectively migrating cells have been shown to move along principal stress directions – a behavior that arises from physical interactions between the cells.⁶⁷ In addition, investigators have recently moved TFM into fully 3D culture models and calculated the forces exerted by both single cells (Fig. 3D)⁶⁹ and engineered epithelial tissues (Fig. 3E)⁷⁰ in these more physiologically relevant environments.

Still, TFM only measures forces at the *boundary* of cells and tissues, not the internal forces transmitted within and between them (Fig. 1B). To probe these internal forces directly, exciting new progress has been made with fluorescence force spectroscopy inside living cells. This technique combines single-molecule fluorescence resonance energy transfer (FRET) with

optical tweezers to determine the forces required to deform flexible linker domains within molecules.^{71,72} These force probes have been primarily used to quantify biomolecular interactions *in vitro*, including protein folding events and movement of motor proteins (Fig. 4A). Recently, however, the probes have been expressed in cultured cells⁷³ and used to measure the mechanical forces across individual molecules within focal adhesions⁷⁴ (Fig. 4B) and adherens junctions^{75,76} (Fig. 4C). Intriguingly, Grashoff and colleagues used a FRET biosensor, which relied on a spider silk-derived, nanospring linker domain,⁷⁷ to calculate the forces across vinculin during focal adhesion assembly.⁷⁴ They reported a force of approximately 2.5 pN in stable focal adhesions, and demonstrated that stabilization was dependent on both force transmission and

vinculin recruitment, processes that were regulated by separate mechanisms.⁷⁴

Ectopically expressed force probes such as these offer distinct advantages over other force probes, like atomic force microscopy, that must be connected mechanically to a measuring instrument,⁷³ since they can probe molecular-level forces inside living cells. Still, there is some uncertainty in how they might be calibrated⁷⁸ – a process that is typically done *in vitro*. Whether the force readouts in a carefully controlled *in vitro* environment are representative of those in the complex environment of living cells is unclear. Moreover, it is assumed that deformations within the FRET force probes are purely one-dimensional, *e.g.* linear tension or compression (*e.g.* Fig. 4A). Any significant deflection or bending of the flexible

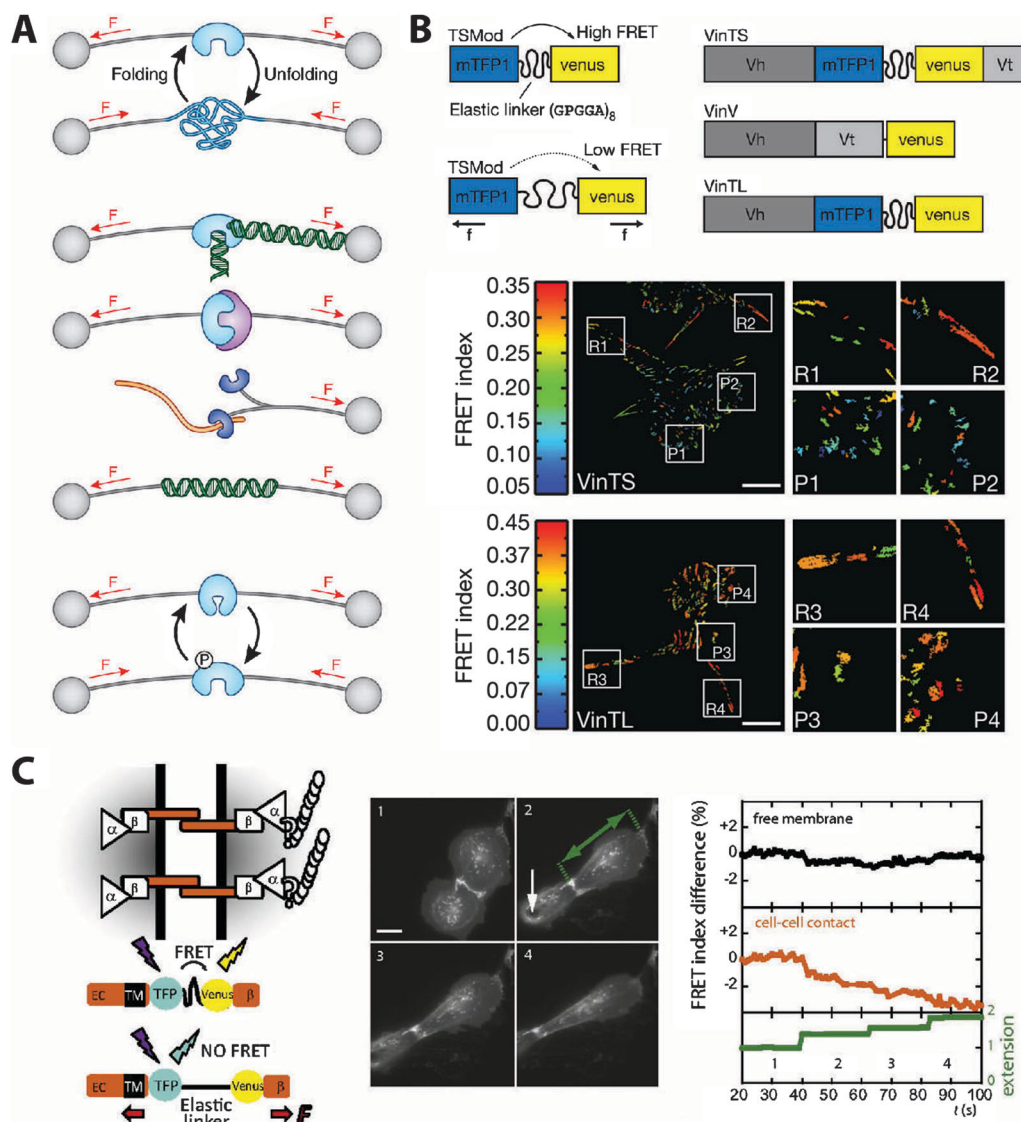


Fig. 4 Fluorescence force spectroscopy inside living cells. (A) Using optical tweezers, small forces can be applied across single molecules. Initially used to characterize biomolecular interactions *in vitro*, this technique has also been employed to calibrate FRET-based force sensors inserted within single molecules of interest. Adapted from de Souza (2012).⁷⁸ Reprinted by permission from Macmillan Publishers Ltd. (B and C) Technique used to calibrate FRET-based force sensors inserted into single molecules and expressed in living cells. Nanospring linker domains introduced into both (B) vinculin and (C) E-cadherin have elucidated forces across focal adhesions and adherens junctions, respectively. Adapted from Grashoff *et al.* (2010)⁷⁴ and Borghi *et al.* (2012).⁷⁵ Reprinted with permission.

linker domain *in vivo* would complicate direct readout of the force.

Despite these questions, endogenous FRET-based force sensors offer enormous potential to measure how forces are transmitted inside living cells. Integrating these techniques with TFM might also reveal how intrinsic and extrinsic forces are coordinated between the intracellular and extracellular environments.

For the first time, advances such as these have made it possible to rigorously quantify the mechanical forces exerted and experienced by cells. It is well established that cells and tissues actively respond to their physical microenvironment, but quantitative descriptions of the feedback mechanisms that underlie this response are lacking. Armed with these tools, however, new quantitative study of these problems is possible.

Probing the viscoelastic response of biological materials

Forces and deformations are coupled through the mechanical properties of a material (Fig. 1C). For typical engineering materials, mechanical properties are determined experimentally using specialized testing equipment such as a rheometer. Importantly, these experiments often require rather large samples (compared to the length scales relevant for tissue assembly). In addition, biological materials change over time, so new methods capable of characterizing the evolving mechanical properties of small biological samples are needed.⁷⁹ To meet this goal, microrheological techniques have emerged as intriguing candidates to probe the viscoelastic properties of biological materials on these small length scales.

Microrheology uses the motion of microscopic particles (~ 0.1 – $1\ \mu\text{m}$ in diameter) to characterize the bulk viscoelastic properties of a material.⁸⁰ In general these properties are frequency-dependent, and the nature of the mechanical response is determined by how quickly the material is deformed. Importantly, the tracer particles probe the material response at the same length scale at which cells physically encounter their microenvironment. This is of particular relevance since many biological materials (*e.g.* collagen gels) undergo nonaffine deformations – that is, deformations at the microscopic level which are distinct from those that occur at a global (or macroscopic) level.⁸¹ These effects are not captured by many traditional mechanical tests which fail to account for microstructural remodeling during deformation.

Broadly, microrheological techniques fall into one of two classes – active or passive. Active methods use external forces such as magnetic fields⁸² or optical tweezers⁸³ to drive particle motion.⁸⁴ Conversely, passive microrheology relies on the thermal excitation of probe particles at equilibrium, and no external physical loads need be applied to the material. This technique was first developed by Mason and Weitz,⁸⁵ who used the generalized Stokes–Einstein equation to relate the average mean squared displacement (MSD) of probe particles embedded in a soft material (see Fig. 5A for example MSDs)

to the complex viscoelastic shear modulus (Fig. 1C). In these initial experiments, the MSD was measured by diffusing wave spectroscopy,⁸⁶ which measured probe motion averaged over a material volume.^{85,87} Unlike traditional rheology, passive microrheology effectively measures a broad range of frequencies simultaneously and probes only the *linear* viscoelastic behavior of the material.⁸⁰

Particle-tracking microrheology later enabled investigators to compute local material properties from the motion of individually tracked beads (Fig. 5B), as opposed to the “bulk” or averaged motion captured by diffusing wave spectroscopy.⁸⁸ This made it possible to compute spatial heterogeneities within a single sample.^{80,89} Moreover, two-point microrheology, which measures the cross-correlated motion of different beads as a function of the distance between them (Fig. 5C), was developed to characterize the macroscopic behavior of materials that are inhomogeneous on the length scale of the probe particles themselves.^{90,91} Owing to these material inhomogeneities, one-point microrheology often fails to capture the viscoelastic properties measured by bulk rheometry (Fig. 5D).⁹²

These innovations are particularly useful for biological materials (such as networks of cytoskeletal or extracellular matrix (ECM) fibers), which are typically small, heterogeneous, and highly viscoelastic^{89,93–95} (Fig. 5D). Only since the invention of microrheology has it been possible to characterize the mechanical properties of these materials at the micrometer length scale. Passive microrheology, however, is constrained to the study of extremely soft materials. Although this technique (conveniently) uses thermal energy to deform the material,⁸⁴ there are practical limits to resolving the thermal motion of the probe particles. For instance, in a purely elastic material, the MSD $\langle \Delta x^2(\tau) \rangle = \langle |x(t + \tau) - x(t)|^2 \rangle$ plateaus with increasing lag time τ and follows the relation⁸⁴

$$\langle \Delta x^2(\tau \rightarrow \infty) \rangle = \frac{k_B T}{\pi G a} \quad (1)$$

where the brackets denote an average over all times t , G is the elastic shear modulus, a is the spherical probe diameter, k_B is Boltzmann’s constant, and T is temperature. For $1\ \mu\text{m}$ -diameter particles embedded in a purely elastic material with $G = 1\ \text{Pa}$, we would estimate particle fluctuations of approximately 30–40 nm at room temperature, which may be lower than the resolution of most imaging methods.

The power of passive microrheology, however, lies in its ability to simultaneously measure both local and global material behavior within an individual specimen. Thus, a wealth of information can be gleaned from a very small amount of sample, which is especially important for biological materials that are either expensive or difficult to isolate in large volumes.⁸⁰

Applied to living cells, active microrheological techniques have suggested that cells in culture behave like a soft glassy material near a glass transition.⁹⁶ Meanwhile, passive measurements in developing *C.elegans* embryos have indicated that the cytoplasm exhibits more liquid-like behavior.⁹⁷ Although these methods enable non-invasive analysis of the mechanics of living cells, passive results must be interpreted carefully.

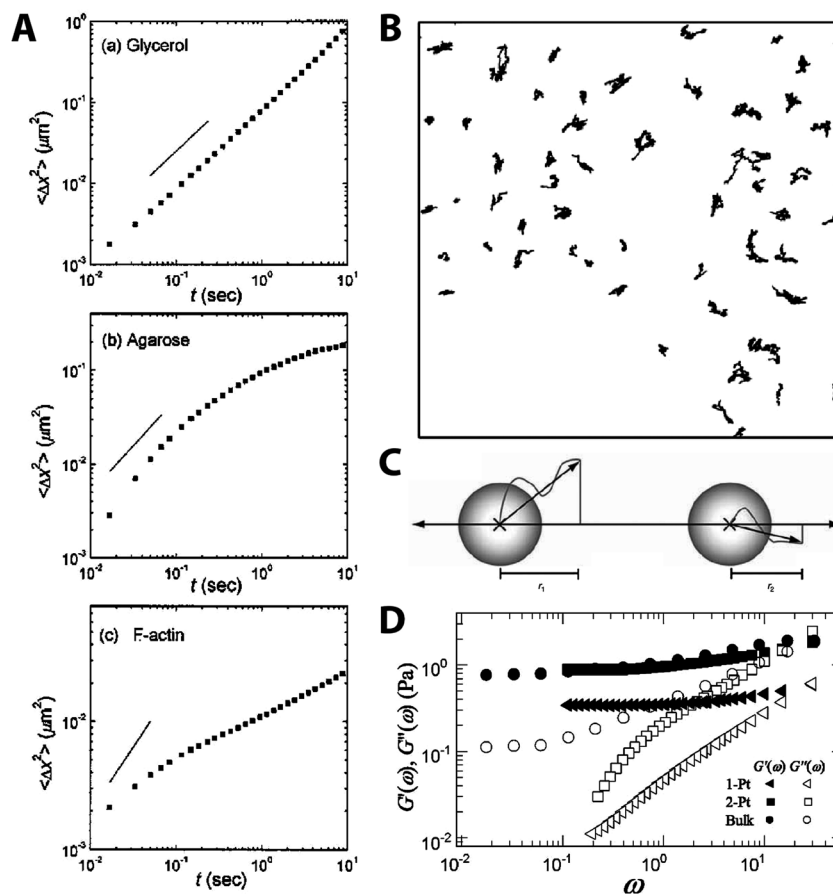


Fig. 5 Probing viscoelastic properties using microrheology. (A) Example time- and ensemble-averaged MSDs for glycerol, agarose, and F-actin. Adapted from Valentine *et al.* (2001).⁸⁹ Reprinted with permission by the American Physical Society. (B) Tracer particle trajectories from particle-tracking microrheology. Adapted from Crocker and Hoffman (2007).⁹¹ Reprinted with permission from Elsevier. (C) Schematic of displacements used to compute cross-correlated motion of neighboring beads for two-point microrheology. Adapted from Crocker and Hoffman (2007).⁹¹ Reprinted with permission from Elsevier. (D) Complex shear modulus of actin-scrutin networks *in vitro* as measured by one- and two-point microrheology, as well as bulk rheology. Given the material inhomogeneity of these networks, one-point microrheology fails to capture the bulk material response, and a two-point approach must be employed. Adapted from Shin *et al.* (2004).⁹⁵ Reprinted with permission.

For instance, the generalized Stokes–Einstein relation assumes that the system is in equilibrium,⁸⁰ which generally is not the case inside the cytoplasm. Still, these tools offer unprecedented access to probing the mechanical responses of cellular and sub-cellular structures.

Micropatterned tissue assembly: bringing it all together

Over the last decade, it has become increasingly clear that cells and tissues adaptively respond to cues from their biochemical and physical microenvironment.⁹⁸ Much of this insight has come from interdisciplinary work that uses the techniques of soft lithography to generate micropatterned tissues of defined geometry in culture. In these assays, elastomeric stamps are fabricated and used to print proteins⁹⁹ or self-assembled monolayers¹⁰⁰ in defined shapes onto 2D surfaces which support cell adhesion^{101,102} (Fig. 6A and B). These patterned adhesive islands offer unprecedented control of tissue geometry,

which has been shown to regulate cell proliferation,¹⁰³ differentiation,¹⁰⁴ and apoptosis^{105,106} in culture.

Given this spatiotemporal control of the tissue micro-environment, micropatterning assays are particularly well suited to investigate the physical cues that direct tissue assembly in culture. These techniques enable the testing of questions that are currently intractable using native tissues.

Recently, micropatterning approaches were extended to create 3D engineered tissues of defined geometry in type I collagen gels (Fig. 6C).¹⁰⁷ Elastomeric stamps were used to mold wells of defined geometry in 3D collagen gels, and cells seeded into these cavities formed organotypic tissues.¹⁰⁸ Using this technique, engineered mammary epithelial tubules have been shown to branch at locations determined by the micropatterned tissue geometry.¹⁰⁷ Moreover, these branching sites were defined by spatially controlled gradients in both morphogen signaling¹⁰⁷ and mechanical stress.^{16,70}

Using many of the disruptive technologies outlined above, this work could be extended to estimate how evolving patterns of mechanical stress regulate branched tissue assembly (Fig. 7).

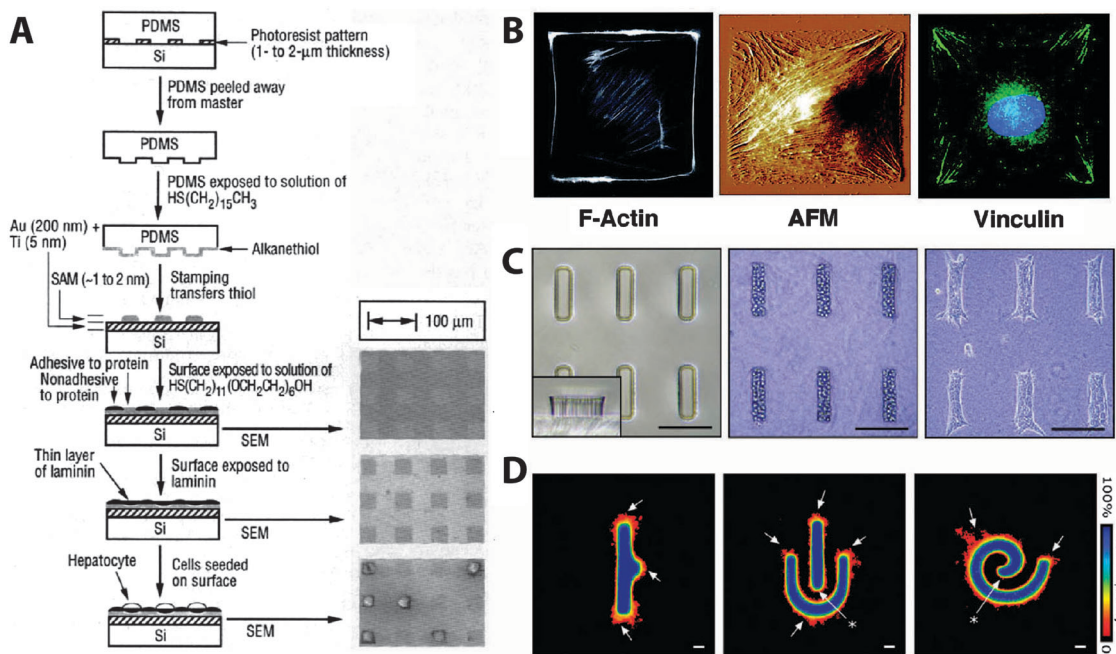


Fig. 6 Micropatterned tissues in 2D and 3D. (A) Schematic for the fabrication of 2D micropatterned tissues by contact printing. Adapted from Singhvi *et al.* (1994).¹⁰¹ Reprinted with permission from AAAS. (B) Organization of stress fibers and focal adhesions in cells cultured on square micropatterned islands. Adapted from Parker *et al.* (2002).¹⁰² Reprinted with permission. (C) Micromolding organotypic epithelial tissues of defined geometry in 3D collagen gels. Adapted from Nelson *et al.* (2008).¹⁰⁸ Reprinted with permission from Macmillan Publishers Ltd. (D) Patterns of mechanical stress dictate branching locations in engineered mammary epithelial tissues. Adapted from Gjorevski and Nelson (2010).¹⁶ Reprinted with permission.

LSM would circumvent the phototoxicity issues that attenuate branching, yet still resolve the 3D morphology of the branching tissues as well as the structure of the surrounding collagen network. Microrheological approaches could be used to assess how spatial variations in the mechanical properties of the gel arise

during branching. If the gel is too stiff, however, active methods such as optical tweezers may be necessary. In addition, FRET force sensors for vinculin or cadherin (or other molecules) could be expressed in these tissues to determine dynamic forces across focal adhesions or adherens junctions in extending branches. Alternatively, force probes inserted into the surrounding ECM proteins¹⁰⁹ would enable FRET-based TFM. Experiments such as these would further advance our understanding of the role that mechanical feedback plays in branched tissue assembly.

Conclusions

Disruptive technologies fundamentally alter how scientific problems are perceived, and often transform the manner in which they might be studied. Such techniques often arise serendipitously – some entirely by chance (*e.g.*, Oliver Smithie's invention of starch-gel electrophoresis¹¹⁰), others by a clever repurposing of things found in nature (*e.g.*, green fluorescent protein,¹¹¹ GFP). The discovery of GFP, for instance, paved the way for live imaging of fluorescently tagged proteins, which ushered in new era of molecular cell biology. Unobservable cellular mysteries all at once made visible.

The field of mechanobiology was born out of observations that cells actively respond to and influence their physical microenvironment. These results have clear implications for medicine and tissue engineering, and new disruptive technologies are helping us move beyond qualitative descriptions towards a more quantitative understanding of the mechanics of tissue assembly.

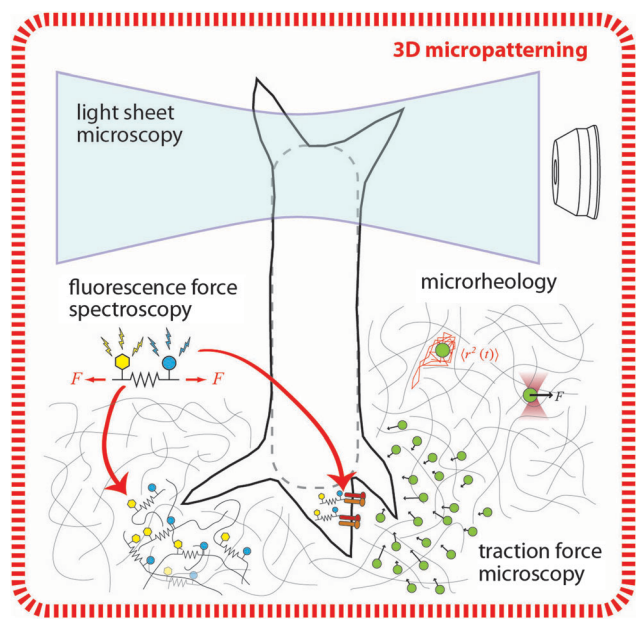


Fig. 7 Light sheet microscopy, traction force microscopy, fluorescence force spectroscopy and microrheology can be combined to study the mechanics of branching morphogenesis in micropatterned 3D epithelial tissues.

Abbreviations

2D	Two-dimensional
3D	Three-dimensional
ECM	Extracellular matrix
FRET	Fluorescence resonance energy transfer
LSM	Light sheet microscopy
MSD	Mean squared displacement
OCT	Optical coherence tomography
PIV	Particle image velocimetry
TFM	Traction force microscopy

Acknowledgements

We thank Jason Gleghorn for his critical reading of the manuscript. Work from the author's group was supported in part by grants from the NIH (GM083997 and HL110335), the David & Lucile Packard Foundation, the Alfred P. Sloan Foundation, and the Camille & Henry Dreyfus Foundation. C.M.N. holds a Career Award at the Scientific Interface from the Burroughs Wellcome Fund.

References

- 1 S. F. Gilbert, *Developmental biology*, Sinauer Associates, 9th edn, 2010.
- 2 D. E. Ingber, V. C. Mow, D. Butler, L. Niklason, J. Huard, J. Mao, I. Yannas, D. Kaplan and G. Vunjak-Novakovic, *Tissue Eng.*, 2006, **12**, 3265–3283.
- 3 T. M. Holder, D. T. Cloud, J. E. Lewis and G. P. Pilling, *Pediatrics*, 1964, **34**, 542–549.
- 4 J. D. Watson and F. H. Crick, *Nature*, 1953, **171**, 737–738.
- 5 E. H. Davidson, J. P. Rast, P. Oliveri, A. Ransick, C. Calestani, C.-H. Yuh, T. Minokawa, G. Amore, V. Hinman, C. Arenas-Mena, O. Otim, C. T. Brown, C. B. Livi, P. Y. Lee, R. Revilla, A. G. Rust, Z. j. Pan, M. J. Schilstra, P. J. C. Clarke, M. I. Arnone, L. Rowen, R. A. Cameron, D. R. McClay, L. Hood and H. Bolouri, *Science*, 2002, **295**, 1669–1678.
- 6 E. H. Davidson, *Nature*, 2010, **468**, 911–920.
- 7 M. S. Hutson and X. Ma, *Phys. Biol.*, 2008, **5**, 015001.
- 8 T. Mammoto and D. E. Ingber, *Development*, 2010, **137**, 1407–1420.
- 9 M. A. Wozniak and C. S. Chen, *Nat. Rev. Mol. Cell Biol.*, 2009, **10**, 34–43.
- 10 S. W. Grill, *Curr. Opin. Genet. Dev.*, 2011, **21**, 647–652.
- 11 G. B. Blanchard and R. J. Adams, *Curr. Opin. Genet. Dev.*, 2011, **21**, 653–663.
- 12 L. A. Davidson, M. A. Koehl, R. Keller and G. F. Oster, *Development*, 1995, **121**, 2005–2018.
- 13 M. S. Hutson, Y. Tokutake, M. S. Chang, J. W. Bloor, S. Venakides, D. P. Kiehart and G. S. Edwards, *Science*, 2003, **300**, 145–149.
- 14 M. Rauzi, P. Verant, T. Lecuit and P. F. Lenne, *Nat. Cell Biol.*, 2008, **10**, 1401–1410.
- 15 V. D. Varner, D. A. Voronov and L. A. Taber, *Development*, 2010, **137**, 3801–3811.
- 16 N. Gjorevski and C. M. Nelson, *Integr. Biol.*, 2010, **2**, 424–434.
- 17 C.-L. Guo, M. Ouyang, J.-Y. Yu, J. Maslov, A. Price and C.-Y. Shen, *Proc. Natl. Acad. Sci. U. S. A.*, 2012, **109**, 5576–5582.
- 18 M. Bathe, C. Heussinger, M. M. A. E. Claessens, A. R. Bausch and E. Frey, *Biophys. J.*, 2008, **94**, 2955–2964.
- 19 J. D. Humphrey, *Cardiovascular solid mechanics: cells, tissues, and organs*, Springer, 2002.
- 20 L. A. Taber, *Nonlinear theory of elasticity: applications in biomechanics*, World Scientific, 2004.
- 21 S. G. Megason and S. E. Fraser, *Cell*, 2007, **130**, 784–795.
- 22 H. Siedentopf and R. Zsigmondy, *Ann. Phys.*, 1903, **315**, 1–39.
- 23 P. J. Keller and H. U. Dodt, *Curr. Opin. Neurobiol.*, 2012, **22**, 138–143.
- 24 R. Tomer, K. Khairy, F. Amat and P. J. Keller, *Nat. Methods*, 2012, **9**, 755–763.
- 25 U. Krzic, S. Gunther, T. E. Saunders, S. J. Streichan and L. Hufnagel, *Nat. Methods*, 2012, **9**, 730–733.
- 26 B. A. Filas, V. D. Varner, D. A. Voronov and L. A. Taber, *J. Visualized Exp.*, 2011, e3129.
- 27 J. Huisken, J. Swoger, F. Del Bene, J. Wittbrodt and E. H. Stelzer, *Science*, 2004, **305**, 1007–1009.
- 28 P. J. Keller, A. D. Schmidt, J. Wittbrodt and E. H. Stelzer, *Science*, 2008, **322**, 1065–1069.
- 29 P. J. Keller, A. D. Schmidt, A. Santella, K. Khairy, Z. Bao, J. Wittbrodt and E. H. Stelzer, *Nat. Methods*, 2010, **7**, 637–642.
- 30 B. A. Filas, A. K. Knutsen, P. V. Bayly and L. A. Taber, *J. Biomech. Eng.*, 2008, **130**, 061010.
- 31 C. Cui, C. D. Little and B. J. Rongish, *Anat. Rec.*, 2009, **292**, 557–561.
- 32 J. Gros, K. Feistel, C. Viebahn, M. Blum and C. J. Tabin, *Science*, 2009, **324**, 941–944.
- 33 D. Huang, E. A. Swanson, C. P. Lin, J. S. Schuman, W. G. Stinson, W. Chang, M. R. Hee, T. Flotte, K. Gregory, C. A. Puliafito and J. G. Fujimoto, *Science*, 1991, **254**, 1178–1181.
- 34 B. A. Filas, I. R. Efimov and L. A. Taber, *Anat. Rec.*, 2007, **290**, 1057–1068.
- 35 C.-Y. Chen, P. G. Menon, W. Kowalski and K. Pekkan, *Exp. Fluids*, 2012, **54**, 1–9.
- 36 I. V. Larina, N. Sudheendran, M. Ghosn, J. Jiang, A. Cable, K. V. Larin and M. E. Dickinson, *J. Biomed. Opt.*, 2008, **13**, 060506.
- 37 A. H. Roeder, A. Cunha, M. C. Burl and E. M. Meyerowitz, *Development*, 2012, **139**, 3071–3080.
- 38 K. Short, M. Hodson and I. Smyth, *Development*, 2013, **140**, 471–478.
- 39 G. B. Blanchard, A. J. Kabla, N. L. Schultz, L. C. Butler, B. Sanson, N. Gorfinkiel, L. Mahadevan and R. J. Adams, *Nat. Methods*, 2009, **6**, 458–464.
- 40 C. M. Nelson and J. P. Gleghorn, *Annu. Rev. Biomed. Eng.*, 2012, **14**, 129–154.

- 41 Y. C. Fung, *Biomechanics: mechanical properties of living tissues*, Springer-Verlag, 2nd edn, 1993.
- 42 K. Langer, *Br. J. Plast. Surg.*, 1978, **31**, 93–106.
- 43 J. D. Humphrey, *J. Biomech. Eng.*, 2001, **123**, 638–641.
- 44 V. D. Varner and L. A. Taber, in *IUTAM symposium on cellular, molecular and tissue mechanics*, ed. K. Garikipati and E. M. Arruda, Springer Netherlands, 2010, vol. 16, pp. 45–54.
- 45 K. A. Beningo and Y. L. Wang, *Trends Cell Biol.*, 2002, **12**, 79–84.
- 46 A. K. Harris, P. Wild and D. Stopak, *Science*, 1980, **208**, 177–179.
- 47 E. Cerda and L. Mahadevan, *Phys. Rev. Lett.*, 2003, **90**, 074302.
- 48 T. Oliver, K. Jacobson and M. Dembo, *Methods Enzymol.*, 1998, **298**, 497–521.
- 49 J. Lee, M. Leonard, T. Oliver, A. Ishihara and K. Jacobson, *J. Cell Biol.*, 1994, **127**, 1957–1964.
- 50 T. Oliver, M. Dembo and K. Jacobson, *Cell Motil. Cytoskeleton*, 1995, **31**, 225–240.
- 51 M. Dembo, T. Oliver, A. Ishihara and K. Jacobson, *Biophys. J.*, 1996, **70**, 2008–2022.
- 52 M. Dembo and Y. L. Wang, *Biophys. J.*, 1999, **76**, 2307–2316.
- 53 S. Munevar, Y. Wang and M. Dembo, *Biophys. J.*, 2001, **80**, 1744–1757.
- 54 R. J. Pelham Jr. and Y. Wang, *Proc. Natl. Acad. Sci. U. S. A.*, 1997, **94**, 13661–13665.
- 55 J. L. Tan, J. Tien, D. M. Pirone, D. S. Gray, K. Bhadriraju and C. S. Chen, *Proc. Natl. Acad. Sci. U. S. A.*, 2003, **100**, 1484–1489.
- 56 O. du Roure, A. Saez, A. Buguin, R. H. Austin, P. Chavrier, P. Silberzan and B. Ladoux, *Proc. Natl. Acad. Sci. U. S. A.*, 2005, **102**, 2390–2395.
- 57 Y. Cai, N. Biais, G. Giannone, M. Tanase, G. Jiang, J. M. Hofman, C. H. Wiggins, P. Silberzan, A. Buguin, B. Ladoux and M. P. Sheetz, *Biophys. J.*, 2006, **91**, 3907–3920.
- 58 N. J. Sniadecki and C. S. Chen, in *Methods in Cell Biology: Cell Mechanics*, ed. W. Yu-Li and E. D. Dennis, Academic Press, 2007, vol. 83, pp. 313–328.
- 59 J. M. Gere, *Mechanics of materials*, Brooks/Cole, 5th edn, 2001.
- 60 Y. Xiang and D. A. LaVan, *Appl. Phys. Lett.*, 2007, **90**, 133901.
- 61 I. Schoen, W. Hu, E. Klotzsch and V. Vogel, *Nano Lett.*, 2010, **10**, 1823–1830.
- 62 S. A. Maskarinec, C. Franck, D. A. Tirrell and G. Ravichandran, *Proc. Natl. Acad. Sci. U. S. A.*, 2009, **106**, 22108–22113.
- 63 J. Chen, J. Irianto, S. Inamdar, P. Pravincumar, D. A. Lee, D. L. Bader and M. M. Knight, *Biophys. J.*, 2012, **103**, 1188–1197.
- 64 W. R. Legant, C. K. Choi, J. S. Miller, L. Shao, L. Gao, E. Betzig and C. S. Chen, *Proc. Natl. Acad. Sci. U. S. A.*, 2013, **110**, 881–886.
- 65 S. S. Hur, Y. Zhao, Y. S. Li, E. Botvinick and S. Chien, *Cell. Mol. Bioeng.*, 2009, **2**, 425–436.
- 66 C. Franck, S. Hong, S. A. Maskarinec, D. A. Tirrell and G. Ravichandran, *Exp. Mech.*, 2007, **47**, 427–438.
- 67 D. T. Tambe, C. C. Hardin, T. E. Angelini, K. Rajendran, C. Y. Park, X. Serra-Picamal, E. H. Zhou, M. H. Zaman, J. P. Butler, D. A. Weitz, J. J. Fredberg and X. Trepapat, *Nat. Mater.*, 2011, **10**, 469–475.
- 68 X. Trepapat, M. R. Wasserman, T. E. Angelini, E. Millet, D. A. Weitz, J. P. Butler and J. J. Fredberg, *Nat. Phys.*, 2009, **5**, 426–430.
- 69 W. R. Legant, J. S. Miller, B. L. Blakely, D. M. Cohen, G. M. Genin and C. S. Chen, *Nat. Methods*, 2010, **7**, 969–971.
- 70 N. Gjorevski and C. M. Nelson, *Biophys. J.*, 2012, **103**, 152–162.
- 71 S. Hohng, R. Zhou, M. K. Nahas, J. Yu, K. Schulten, D. M. Lilley and T. Ha, *Science*, 2007, **318**, 279–283.
- 72 F. Meng, T. M. Suchyna and F. Sachs, *FEBS J.*, 2008, **275**, 3072–3087.
- 73 Y. F. Dufrene, E. Evans, A. Engel, J. Helenius, H. E. Gaub and D. J. Muller, *Nat. Methods*, 2011, **8**, 123–127.
- 74 C. Grashoff, B. D. Hoffman, M. D. Brenner, R. Zhou, M. Parsons, M. T. Yang, M. A. McLean, S. G. Sligar, C. S. Chen, T. Ha and M. A. Schwartz, *Nature*, 2010, **466**, 263–266.
- 75 N. Borghi, M. Sorokina, O. G. Shcherbakova, W. I. Weis, B. L. Pruitt, W. J. Nelson and A. R. Dunn, *Proc. Natl. Acad. Sci. U. S. A.*, 2012, **109**, 12568–12573.
- 76 D. E. Conway, M. T. Breckenridge, E. Hinde, E. Gratton, C. S. Chen and M. A. Schwartz, *Curr. Biol.*, 2013, **23**, 1024–1030.
- 77 N. Becker, E. Oroudjev, S. Mutz, J. P. Cleveland, P. K. Hansma, C. Y. Hayashi, D. E. Makarov and H. G. Hansma, *Nat. Mater.*, 2003, **2**, 278–283.
- 78 N. de Souza, *Nat. Methods*, 2012, **9**, 873–877.
- 79 K. E. Kasza, A. C. Rowat, J. Liu, T. E. Angelini, C. P. Brangwynne, G. H. Koenderink and D. A. Weitz, *Curr. Opin. Cell Biol.*, 2007, **19**, 101–107.
- 80 T. M. Squires and T. G. Mason, *Annu. Rev. Fluid Mech.*, 2010, **42**, 413–438.
- 81 E. A. Sander, T. Stylianopoulos, R. T. Tranquillo and V. H. Barocas, *Proc. Natl. Acad. Sci. U. S. A.*, 2009, **106**, 17675–17680.
- 82 F. Ziemann, J. Rädler and E. Sackmann, *Biophys. J.*, 1994, **66**, 2210–2216.
- 83 D. Velegol and F. Lanni, *Biophys. J.*, 2001, **81**, 1786–1792.
- 84 M. L. Gardel, M. T. Valentine and D. A. Weitz, in *Microscale Diagnostic Techniques*, ed. K. S. Breuer, Springer, New York, 2005, pp. 1–50.
- 85 T. G. Mason and D. A. Weitz, *Phys. Rev. Lett.*, 1995, **74**, 1250–1253.
- 86 D. J. Pine, D. A. Weitz, P. M. Chaikin and E. Herbolzheimer, *Phys. Rev. Lett.*, 1988, **60**, 1134–1137.
- 87 T. G. Mason, H. Gang and D. A. Weitz, *J. Opt. Soc. Am. A*, 1997, **14**, 139–149.
- 88 T. G. Mason, K. Ganesan, J. H. van Zanten, D. Wirtz and S. C. Kuo, *Phys. Rev. Lett.*, 1997, **79**, 3282–3285.

- 89 M. T. Valentine, P. D. Kaplan, D. Thota, J. C. Crocker, T. Gisler, R. K. Prud'homme, M. Beck and D. A. Weitz, *Phys. Rev. E*, 2001, **64**, 061506.
- 90 J. C. Crocker, M. T. Valentine, E. R. Weeks, T. Gisler, P. D. Kaplan, A. G. Yodh and D. A. Weitz, *Phys. Rev. Lett.*, 2000, **85**, 888–891.
- 91 J. C. Crocker and B. D. Hoffman, *Methods Cell Biol.*, 2007, **83**, 141–178.
- 92 A. J. Levine and T. C. Lubensky, *Phys. Rev. Lett.*, 2000, **85**, 1774–1777.
- 93 F. Gittes, B. Schnurr, P. D. Olmsted, F. C. MacKintosh and C. F. Schmidt, *Phys. Rev. Lett.*, 1997, **79**, 3286–3289.
- 94 J. Apgar, Y. Tseng, E. Fedorov, M. B. Herwig, S. C. Almo and D. Wirtz, *Biophys. J.*, 2000, **79**, 1095–1106.
- 95 J. H. Shin, M. L. Gardel, L. Mahadevan, P. Matsudaira and D. A. Weitz, *Proc. Natl. Acad. Sci. U. S. A.*, 2004, **101**, 9636–9641.
- 96 B. Fabry, G. N. Maksym, J. P. Butler, M. Glogauer, D. Navajas and J. J. Fredberg, *Phys. Rev. Lett.*, 2001, **87**, 148102.
- 97 B. R. Daniels, B. C. Masi and D. Wirtz, *Biophys. J.*, 2006, **90**, 4712–4719.
- 98 C. M. Nelson, *Biochim. Biophys. Acta*, 2009, **1793**, 903–910.
- 99 R. S. Kane, S. Takayama, E. Ostuni, D. E. Ingber and G. M. Whitesides, *Biomaterials*, 1999, **20**, 2363–2376.
- 100 K. L. Prime and G. M. Whitesides, *Science*, 1991, **252**, 1164–1167.
- 101 R. Singhvi, A. Kumar, G. P. Lopez, G. N. Stephanopoulos, D. I. Wang, G. M. Whitesides and D. E. Ingber, *Science*, 1994, **264**, 696–698.
- 102 K. K. Parker, A. L. Brock, C. Brangwynne, R. J. Mannix, N. Wang, E. Ostuni, N. A. Geisse, J. C. Adams, G. M. Whitesides and D. E. Ingber, *FASEB J.*, 2002, **16**, 1195–1204.
- 103 C. M. Nelson, R. P. Jean, J. L. Tan, W. F. Liu, N. J. Sniadecki, A. A. Spector and C. S. Chen, *Proc. Natl. Acad. Sci. U. S. A.*, 2005, **102**, 11594–11599.
- 104 E. W. Gomez, Q. K. Chen, N. Gjorevski and C. M. Nelson, *J. Cell. Biochem.*, 2010, **110**, 44–51.
- 105 C. S. Chen, M. Mrksich, S. Huang, G. M. Whitesides and D. E. Ingber, *Science*, 1997, **276**, 1425–1428.
- 106 C. S. Chen, M. Mrksich, S. Huang, G. M. Whitesides and D. E. Ingber, *Biotechnol. Prog.*, 1998, **14**, 356–363.
- 107 C. M. Nelson, M. M. Vanduijn, J. L. Inman, D. A. Fletcher and M. J. Bissell, *Science*, 2006, **314**, 298–300.
- 108 C. M. Nelson, J. L. Inman and M. J. Bissell, *Nat. Protocols*, 2008, **3**, 674–678.
- 109 W. R. Legant, C. S. Chen and V. Vogel, *Integr. Biol.*, 2012, **4**, 1164–1174.
- 110 O. Smithies, in *Methods in Molecular Biology: Protein Electrophoresis*, ed. B. T. Kurien and R. H. Scofield, Humana Press, 2012, vol. 869, pp. 1–21.
- 111 O. Shimomura, *J. Microsc.*, 2005, **217**, 3–15.